COBEM 2023 27TH INTERNATIONAL CONGRESS OF MECHANICAL ENGENEERING

ABCM Brazilian Society of Mechanical Sciences and Engineering
27th ABCM International Congress of Mechanical Engineering
December 04-08, 2023, Florianópolis-SC, Brazil

# COB-2023-1496 TWO-AXIS SOLAR TRACKER FOR OFFSET PARABOLIC-DISH SOLAR CONCENTRATORS

**George Orbezo Alvarez**
**Vicente Luiz Scalon**
São Paulo State University (Unesp), School of Engineering, Bauru. Av. Eng. Luiz Edmundo C. Coube, 14-01, 17033-360 Bauru, São Paulo, Brazil.
george.orbezo@unesp.br, vicente.scalon@unesp.br

**Alexandre Duarte**
**Daniel Villas Bôas**
**Elí Wilfredo Zavaleta Aguilar**
São Paulo State University (Unesp), School of Engineering, Itapeva. Rua Geraldo Alckmin, 519, 18409-010 Itapeva, São Paulo, Brazil.
alexandre.duarte@unesp.br, daniel.villas@unesp.br, eli.zavaleta@unesp.br

***Abstract.*** *Due to the climate crisis, there is a worldwide need to decarbonize industries to achieve zero emissions targets by 2050. In Brazil, heat in industries is responsible for 80% of energy demand, of which 53% comes from fossil sources. In addition, 41% of industrial processes use temperatures above 400 °C, which can be supplied by solar collectors with concentration and solar two-axis tracking systems. Two-axis solar tracking allows the concentrator to follow the sun throughout the day. This work aims to design, build, program, and evaluate the performance of two closed-loop solar tracking systems, consisting of 4 LDR sensors, an Arduino board, an ESP32-CAM board, two DC motors, two H-bridges, two-speed reduction gears, and angle sensors (MPU6050 and HMC5883L). The first solar tracking system is managed by LDR sensors and the second by image recognition. The comparison is given by measuring the solar azimuth and elevation angles by HMC5883L and MPU6050 sensors, respectively, which are compared with the theoretical ones. The first system shows an RMSE error of 2.10° for the elevation angle and 10.74° for the azimuth angle. The second system shows an RMSE error of 1.98° for the elevation angle and 6.68° for the azimuth angle, achieving an improvement with respect to the first system.*

***Keywords:*** *Parabolic dish, solar concentration, automation, industry, heating.*

## 1. INTRODUCTION

Solar energy is the largest available energy source in the world, surpassing by 25 times (in one year) the total extractable reserves of coal and by 1200 times the total energy used in the world (IEA, 2015). This fact encourages research into its use, although there are some difficulties, such as seasonality, clouds, lack of use at night and low energy density where even outside the atmosphere, it is 1367 W/m² (Duffie and Beckman, 2013) and decreases further due to scattering and absorption effects in the atmosphere until its arrival on the earth's surface. The two technologies most used for its use are photovoltaic and thermal. Solar thermal energy consists of transforming solar radiation into heating materials (solids, liquids, or gasses) using solar thermal collectors, which can heat these materials up to more than 1000 °C depending on the collector technology. For medium and high temperatures (> 400 °C), the collector must have a concentrator, which is basically a surface that concentrates the radiation in small areas. On the other hand, in Brazil, it was identified (Solar Payback, 2017) that in the industrial sector, heat is responsible for 2.82 EJ (80%) of the energy demand, which 53% of this energy comes from fossil sources, and 41% of the heat in industries uses temperatures above from 400 °C. Thus, there is the possibility of using solar energy for industrial processes and thereby achieving zero carbon targets by 2050.

To achieve temperatures > 400 °C in the receiver, the collector must have a concentrator; in addition, the concentrator must have a solar tracking system since most concentrators, such as the parabolic dish, Scheffler or the solar tower, work with the direct solar radiation. There are several methodologies for solar tracking, which can be classified according to the rotation of the axis, type of drive and control scheme. (Musa et al., 2023) classified solar tracking systems according to the number of axes and the type of axis rotation, such as rotation in a single axis (VSAT, HSAT, TSAT and PASAT), in two axes ((TTDAT and AADAT) and hybrid. Vertical single-axis trackers (VSAT) track the azimuth by rotating the vertical axis from east to west throughout the day. (Lorenzo et al., 2002) achieved a gain of up to 40% in photovoltaic systems compared to static-inclined ones. Horizontal single-axis trackers (HSAT) try to approximate the inclination of the plate to the solar elevation (Li et al., 2012) evaluated that an HSAT system with a north-south axis captured 36% more energy than if it was positioned with an east-west axis. Tilted single-axis trackers (TSAT) have their axis of rotation tilted. Finally, polar-aligned single-axis trackers (PASAT) are the same as TSATs with the difference that the former have their

axis aligned with the Pole Star, which is parallel to the north-south axis of the earth (Li & Lam, 2007). On the other hand, there are dual-axis solar tracking systems, which allow more solar radiation to be captured than those with one axis due to their more complete tracking. These solar trackers can be of the tip-tilt dual-axis tracking (TTDAT) type and azimuth-altitude dual-axis trackers (AADAT). In TTDAT, the structure to rotate is at the top of a vertical fixed pole. For its part, the AADAT tracker generally has a large ring on the ground where it distributes the weight of the structure. The ring allows it to follow the azimuth angle (Reda & Andreas, 2008). There is also a hybrid or three-axis solar tracker, where in addition to two-axis tracking, a third axe is added that allows the structure to be raised and lowered to avoid shady areas (Gupta et al., 2022). According to (Musa et al., 2023), the system with one axis is the cheapest, the hybrid the most complex, expensive, and precise, followed by the one with two axes.

Another classification is based on the drive types, which includes passive, active and chronological systems. The passive system does not use electrical devices, its movement being directed by counterweights. It is low cost, easy to repair, but less accurate. In addition, it has a lateral damper that prevents sudden movements due to wind or other sources (Corp Z, 2014). The active systems use motors and gear trains to align the solar tracker in the direction of the sun with one, two or more axes. Compared to passive trackers, active trackers are more expensive but provide higher accuracy requiring regular maintenance due to motors and moving parts (Musa et al., 2023). These systems use light sensors to track the sun. On the other hand, the chronological system uses geographic coordinates and astronomical knowledge to find the sun's location. Its drawback is that this system is affected by the environment and electrical discharges. (Musa et al., 2023) indicate that the most expensive, complex, reliable, and accurate is the active system, followed by the chronological one and finally, the passive one. In low temperatures, the active system can work, unlike the passive system. In addition, the active system can be turned on and off even though there is a windstorm; the chronological one does not work in a windstorm because it can decalibrate the system, which is previously programmed, and the passive one must be manually turned off in windstorms.

The classification based on the control scheme can be closed-loop and open-loop. The closed-loop type is based on feedback control, where input data, such as from light sensors, are manipulated in the controller, and then it produces outputs to drive the motors (Lee et al., 2009). On the other hand, in the open-loop system, the inputs are calculated, and the algorithm moves the motors of the system without using feedback to verify if the objective has been reached. Consequently, an open-loop system cannot correct any errors it might make and does not compensate for disturbances in the system (Mccluney, 1983). The open-loop system is simpler and cheaper than the closed-loop solar tracking system. Table 1 presents some works of dual-axis solar tracking systems.

Table 1. Works related to two-axis solar trackers.

| **Autor** | **Description** |
|---|---|
| Tchao et al. (2022) | Solar tower. Camera, one vertical axis with shadow (vision controller), 1 Arduino Uno, 2 stepper motors, 4 LDRs. Error: $\alpha_e = 0.887°$, $\gamma_{s,e} = 0.801°$ |
| Mohanapriya et al. (2021) | PV. Arduino Uno, 4 LDR, 2 stepper motors. $\Delta\eta = 30 – 40\%$. |
| Rajasekaran et al. (2021) | PV. 4 LDR, 2 stepper motors, 1 Arduino Uno, 1 position sensor, 1 LCD. $\Delta\eta = 20 – 30\%$. |
| Hamad et al., (2020) | PV. 1 Arduino Mega 2560, 4 LDR, 2 servo motors (controlled by PWM), 1 ACS712, 1 LCD, 1 Bluetooth module HC-05. $\Delta\eta = 20\%$. |
| Imron et al., (2020) | PV. 4 LDR, 1 Arduino ATMega 16, 2 12V DC motors. $\Delta\eta = 30\%$. |
| Gajjar (2017) | PV. 1 12 V DC electrical control with track and tilt circuit, 4 LDRs, 2 motors. $\Delta\eta = 17.53\%$. |
| Medeiros (2016) | PV. 1 Arduino Uno, 2 servo motors SG90, 2 batteries Li-Po 3.7V, 4 LDR. $\Delta\eta = 30\%$. |
| Sohag et al. (2015) | PV. Arduino Uno, 4 LDR, 1 2 Megapixel webcam that captures sun images, 2 servo motors. It uses an image processing algorithm. |
| Pradeep et al. (2014) | PV. 1 Arduino Uno, 4 LDR, 2 DC gear reduction motors, LabView software for programming. |
| Ahammed Ferdaus et al. (2013) | PV. 5 LDR, 1 comparator circuit based on LM1458 ICs and diodes, 1 Atmega32, 2 35byj46 geared stepper motors. $\Delta\eta = 52.78\%$. |

| | |
|---|---|
| Zhan et al. (2013) | PV. 1 PLC, 2 DC motors DC. $\Delta\eta = 8 – 25\%$. |

$\alpha_e$ is the elevation angle error, $\gamma_{s,e}$ is the azimuth angle error, PV is photovoltaic and $\Delta\eta$ is the efficiency variation in relation to a fixed PV system.

Because the solar tracking of this work is for a parabolic concentrator, it is necessary that its tracking be of two axes. This work considers a tip-tilt dual-axis tracking (TTDAT). The objective of this work is to compare two low-cost solar trackers, one using LDR sensors and the other, in addition to using LDR sensors, also uses image processing.

## 2. METHODOLOGY

### 2.1 Dish concentrator structure and electronic components

In this work, the reflector of a 60 cm offset parabolic antenna was used. Initially, the antenna reflector was removed, and a structure was built that allowed its movement in two axes. The vertical axis has a small tip at its bottom. The base plate has a small hole where the tip rotates. Externally to the vertical axis, a steel tube of 80 mm ED was placed. The shaft and tube are separated by a plastic ring built on a 3D printer. This ring is positioned at the top of the tube. Vertical and horizontal axes were rotated by 12V DC car glass motors which have 8 teeth gear; no-load, nominal, and motor-locked current of 2.5 A, 7.5 A and 25 A, respectively; nominal and locked torque of 3 Nm, 8 Nm, respectively; no-load and nominal speed of 80 rpm and 65 rpm, respectively. To reduce the vertical shaft rotational speed, an 87:8 gear reduction was added. The horizontal shaft also features a 110:8 gear reduction. The 87 and 110-tooth gears were manufactured using a 3D printer. The 110-tooth gear has an incomplete body so as not to interfere with the reflector. To allow the solar radiation reflection, small square mirrors of 0.5 cm on each side were glued to the inner surface of the reflector. The antenna reflector is offset type; this means that the reflecting surface is not symmetrical with respect to the parabola vertex. Thus, it was determined by measurements and geometric relationships that the opening area for solar radiation is circular with a diameter of 604 mm. Also, the focus of the parabola is 380 mm long from the vertex. Figure 1 shows a schematic of the parabolic surface. The scheme also shows, in blue color, a flat surface that is perpendicular to the parabola axis and direct solar radiation. The flat surface is the base of a shader that consists of two flat walls in a cross shape where luminosity sensors are placed. The shader was manufactured on a 3D printer. The system has two KW12-3 micro switches with a 90° rotation limit, ensuring that there is no interference between components.


(a) (b) (c)

Figure 1. (a) scheme of the satellite dish reflective surface, (b) still picture of the offset parabolic solar tracker and (c) still picture of the LDR sensors placed in the shader.

Some electronic components were used for the parabolic movement control and angular measurements, which were: Arduino ATMega 2560 board, ESP32-CAM, BTS7960 H bridge, GL5528 LDR sensor, HMC5883L magnetometer board and a MPU6050 3-axis gyroscope and accelerometer module.

### 2.2 Operating logic

The Arduino ATMega 2560 board is responsible for making the solar tracker work correctly through the programming done in the Arduino IDE; similarly, the Esp32-CAM microcontroller sends the angle measurement data from the MPU6050 (solar elevation) and HMC5883L (azimuth) sensors to the computer. The mechanism's motors move according to the LDR sensor readings, or the images captured by the ESP32-CAM. The operation logic is represented in the block diagram of Figure 2.

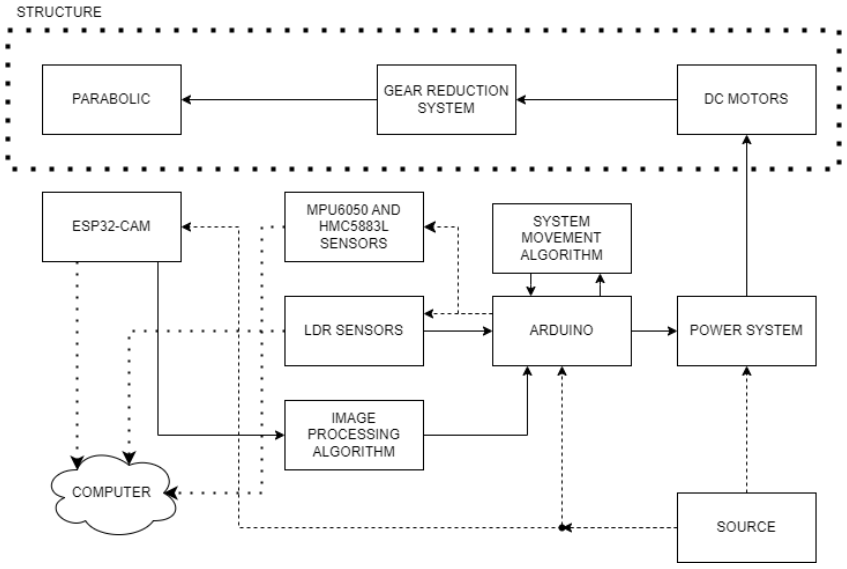


Figure 2. Solar tracker block diagram.

When the mechanism is driven by LDR, the Arduino ATMega 2560 board receives the data read by the 4 LDR sensors located in the shader (Figure 1c), then it performs the difference between the data from the sensors located in the upper and lower part; if that difference is significant, the horizontal shaft will rotate in the elevation angle direction. In a similar way, the board performs the data subtraction of the LDR sensors located in the left and right parts of the shader to move the vertical shaft in the azimuth angle direction. In both cases, the motors are controlled and driven by a H bridge. For the case of the image-driven mechanism, the system moves by the LDR sensors until it faces the sun, then the ESP32-CAM camera takes an image capture and performs image processing using an algorithm that initially converts the image to a grayscale, then use a Gaussian blur to soften the image, then apply a binary threshold to separate the image into two values (light or dark), then a morphological transformation called opening is carried out, which seeks to eliminate the image internal noise. Finally, it performs the function of finding the sun contours and center, as well as the center of the image, which are printed in the image as coordinates in pixel values. This process is shown in Figure 3.

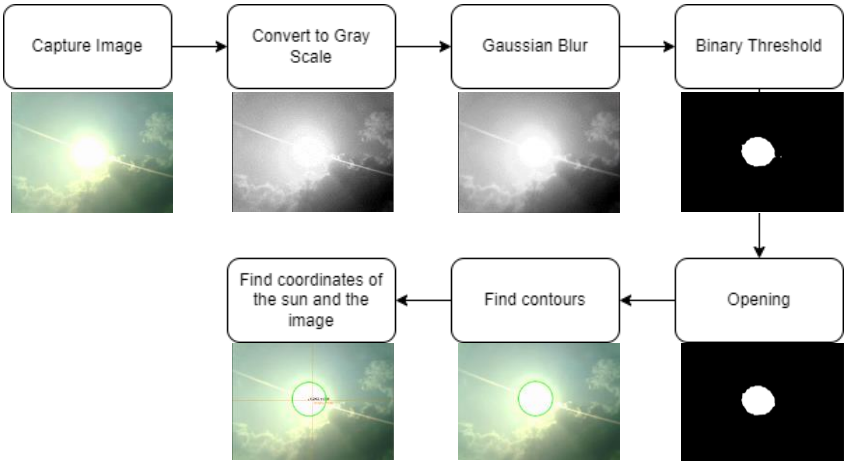


Figure 3. Image processing steps.

The difference in the *x* coordinates between the center of the image and the sun is calculated. If this difference is different of 10 pixels, the azimuth motor rotates the axis to the left or right. Similarly, the difference in *y* coordinates is calculated, rotating the solar elevation axis up or down, if necessary. When there are no more differences, the image being captured by the ESP32-CAM is saved, as well as the values of the MPU6050 and HMC5883L sensors.

## 3. RESULTS

For each test, initially, the elevation and azimuth angles were zero; after that, the system performed solar tracking. Figure 4 shows the parabolic dish pointing to the sun on 06/30/2023 at 4:30 pm in slightly cloudy sky conditions. The

first data measurement was sent to the computer at the first second, and after each time when the motor turned. All data were saved in a CSV file. So, it is possible to have a better visualization of angular variations and measurement system and motor actuation errors.

Figure 4. Parabolic dish axis pointing to the sun.

The data read from the MPU6050 and HMC5883L sensors were processed in the Arduino IDE (programmed in C++) to obtain the solar position angles (solar elevation and azimuth), which were compared with the angles theoretically obtained from (Spencer, 1971) which depend on the latitude, longitude, and time of the place where the experiments were carried out (Unesp/Bauru: 22.3510 S and 49.0348 O). The angles obtained were graphed for better visualization. Figures 5 and 6 show the data for September 19, 2023, using the LDR method. Figure 5 compares the elevation angle calculated by Spencer (1971) and the one measured. Similarly, Figure 6 compares the azimuth angle. The two graphs show that the system rotates with the same tendency as Spencer (1971) angles, but there are oscillations due to the system's inertial movements and the programming sensitivity for the start of the motor drive, furthermore, in Figure 6, it can be seen that the sensor data measured is far from the theoretical value, this is because the system is not built perfectly and because the LDR sensors are not very sensitive in the event that the sky is cloudy. Therefore, the system does not work completely as it should. The errors were calculated by the RMSE (Root-Mean-Square Error) index for the two angles, obtaining values of 2.10° for the elevation angle and 10.74° for the azimuth angle.

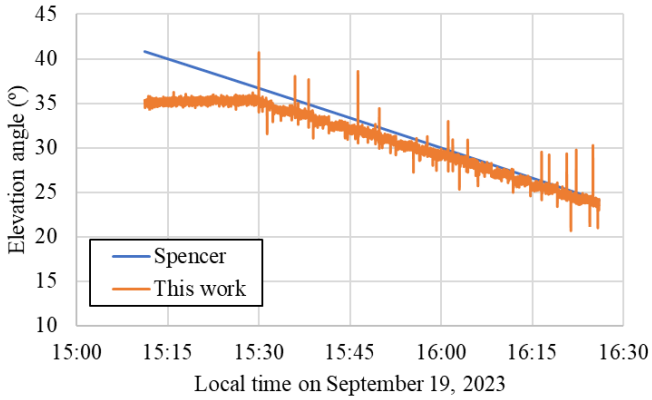


Figure 5. Elevation angles comparison by the LDR method.

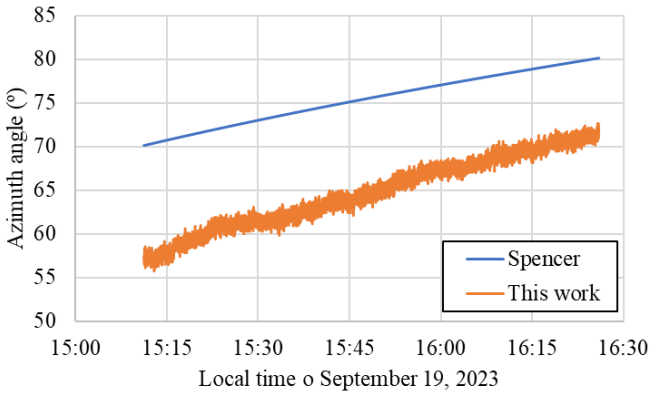


Figure 6. Azimuth angles comparison by the LDR method.

Figures 7 and 8 show the results of the tests carried out using the image-controlled system method. Figure 7 indicates the comparison of the measured solar elevation angle and the one calculated by Spencer (1971). On the other hand, Figure 8 shows the comparison of the azimuth angle. The experiments were carried out on the same place on September 21, 2023. Figures 7 and 8 show that the system rotates with the same trend as the theoretical angles, but an error was found in the measurements, due to the angle sensors precision and because the system is not built perfectly. It is also due to the precision of image processing to find the sun and with that, the system is in oscillation, as seen in Figure 8. The RMSE error index shows 1.98° for the elevation angle and 6.68° for the azimuth angle.

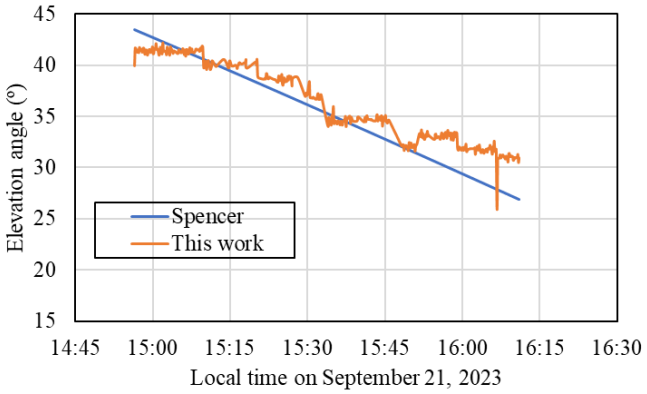


Figure 7. Elevation angle comparison by the image recognition method.

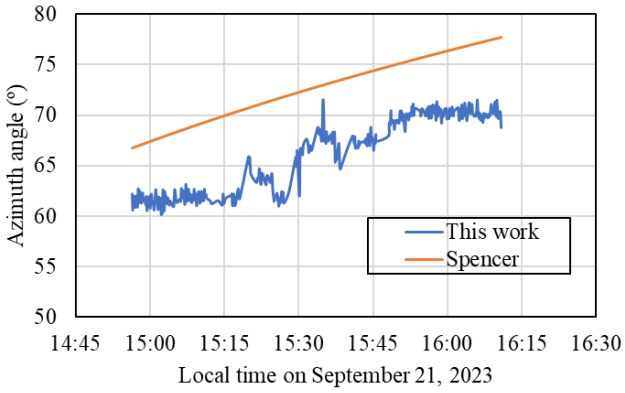


Figure 8. Azimuth angle comparison by the image recognition method.

It can be seen in Figures 6 and 8 that the errors in the azimuth angle are considerable, this is due to the initial reference error (~ 5°), additionally, the system with LDR also has the error due to the test day was cloudy and the sensors were not able to correct the LDRs reading differences.

Finally, Figure 9 shows a comparison between the images captured by the system that uses LDR and the image recognition, the images were taken with seven seconds of difference. The method that uses image recognition captures

the sun better compared to the system that uses LDR. Several tests were carried out and in all of them, it was observed that the image recognition method made a better approximation of the sun, obtaining a centered image as in Figure 9b.

(a) (b)

Figure 10. Comparison between images captured by a) LDR, and b) image processing methods.

## 4. CONCLUSIONS

In this work, a double axis solar tracker has been designed, built, and programmed, which follows the sun trajectory with the help of LDR sensors or image processing. Else, the elevation and azimuth angles were measured to verify the sun position and the system accuracy. The errors obtained using the image recognition method provide lower value compared to the LDR method. Despite being a low-cost system and not be perfectly built, the system with image recognition meets the expectation of following the sun, locating it centrally, and guaranteeing better solar capture. The errors obtained in the measurements of the system managed by LDR sensors are due to the precision of the LDR sensors and the sensitivity of the motors, while the system managed by image recognition is due to the measurement precision of the MPU6050 and HMC8553L sensors and the image processing algorithm precision to find the position of the sun. It is necessary to carry out new tests to correct azimuth angle reading problems.

## 5. REFERENCES

Ahammed, F.R., Rahman, S., Abdul, M.M., and Asif, M. M., 2013. Design & Implementation of a Dual Axis Solar Tracking System. *Academic & Scholarly Research Journal*, Vol. 5, Issue 1.

Corp, Z., 2014. *Photovoltaic tracking racks*. http://www.zomeworks.com/photovoltaic-tracking-racks/

Duffie, J., Beckman, W., 2013. Solar engineering of thermal processes, 4ª Ed., New Jersey: Wiley.

Gajjar, V.K., 2017. An experimental study on dual axis solar tracking system. *International Journal of Mechanical and Production Engineering*, Vol. 5, Issue 5.

Gupta, P., Gupta, V., Sharma, M., Pachauri, R. K., and Akhtar, J., 2022. Design and Performance Analysis of Three axis Solar Tracking System. *Proceedings - 2022 7th Asia Conference on Power and Electrical Engineering, ACPEE 2022*, 1876–1880.

Hamad, B.A., Ibraheem, A.M.T., and Abdullah, A.G., 2020. Design and practical implementation of dual-axis solar tracking system with smart monitoring system. *Przeglad Elektrotechniczny*, Vol. 96, pp. 151–155.

IEA. Solar update, v. 62, 2015. https://www.iea-shc.org/Data/Sites/1/publications/2015-11-Solar-Update-Newsletter.pdf. Accesed 01 fev. 2021.

Imron, C., Abadi, I., Brillianti, N., Khamim, A.M., Ahmad N.Y., and Saepul U.A., 2020. Fuzzy Logic Controller Application for an Active Two-Axis Solar Tracking System. *E3S Web of Conferences, 190*.

Medeiros, I.P.M., 2016. *Sistema de controle rastreável para painéis fotovoltaicos: Protótipo*. MS dissertation, Graduate Program in Mechanical Engineering, Federal University of Rio Grande do Norte, Natal, Brazil.

Lee, C.Y., Chou, P.C., Chiang, C.M., and Lin, C.F., 2009. Sun tracking systems: A review. In *Sensors*, Vol. 9, Issue 5, pp. 3875–3890.

Li, D.H.W., and Lam, T.N.T., 2007. Determining the optimum tilt angle and orientation for solar energy collection based on measured solar radiance data. *International Journal of Photoenergy*, Vol. 2007.

Li, G., Runsheng, T. and Hao, Z., 2012. Optical Performance of Horizontal Single Axis Tracked Solar Panels. In *International Conference on Future Energy, Environment and Materials 16*, pp. 1744–1752.

Lorenzo, E., Pérez, M., Ezpeleta, A., and Acedo, J., 2002. Design of tracking photovoltaic systems with a single vertical axis. *Progress in Photovoltaics: Research and Applications*, Vol. 10, pp. 533–543.

Mccluney, R., 1983. Passive optical solar tracking system. *Applied Optics*, Vol. 22, pp. 3433-3439.

Mohanapriya, V., Manimegalai, V., Praveenkumar, V., and Sakthivel, P., 2021. Implementation of Dual Axis Solar Tracking System. *IOP Conference Series: Materials Science and Engineering*, Vol. 1084, 012073.

Musa, A., Alozie, E., Suleiman, S.A., Ojo, J.A., and Imoize, A. L., 2023. A Review of Time-Based Solar Photovoltaic Tracking Systems. In *Information (Switzerland)*, Vol. 14, Issue 4.

Pradeep, K. P. J., Sai, P.R.K., Chandra M.C., and Nagabhushan R.K., 2014. Development of Dual-Axis Solar Tracking using Arduino with Lab VIEW. *International Journal of Engineering Trends and Technology*, Vol. 17, pp. 321–324.

Solar Payback. Solar thermal energy for industry (in Portuguesse). Solrico, 2017.

Rajasekaran, S., Murugan, P., Selvin, N. T., and Arumuga, B.M., 2021. Design and Development of Dual Axis Solar Tracking System using Arduino. In *Volatiles & Essent. Oils*, Vol. 8, Issue 4.

Reda, I., and Andreas, A., 2008. *Solar Position Algorithm for Solar Radiation Applications (Revised)*. http://www.osti.gov/bridge

Sohag, H.A., Hasan, M., Khatun, M., and Ahmad, M., 2015. An accurate and efficient solar tracking system using image processing and LDR sensor. *2nd International Conference on Electrical Information and Communication Technologies, EICT 2015*, pp. 522–527.

Spencer, J. W., 1971. Fourier Series Representation of the Position of the Sun. *Search*, Vol. 2, pp. 162-172.

Tchao, E.T., Asakipaam, S.A., Fiagbe, Y.A.K., Yeboah-Akowuah, B., Ramde, E., Agbemenu, A.S., and Kommey, B., 2022. An Implementation of an optimized dual-axis solar tracking algorithm for concentrating solar power plants deployment. *Scientific African*, Vol. 16.

Zhan, T.S., Lin, W.M., Tsai, M.H., and Wang, G.S., 2013. Design and implementation of the dual-axis solar tracking system. *Proceedings - International Computer Software and Applications Conference*, pp. 276–277.

## 6. RESPONSIBILITY NOTICE

The authors are the only responsible for the printed material included in this paper.